

## Synthesis and Properties of a Cyclohexa-2,7-anthrylene Ethynylene Derivative

メタデータ	言語: eng 出版者: 公開日: 2020-11-17 キーワード (Ja): キーワード (En): 作成者: Matsuki, Hironori, Okubo, Keisuke, Takaki, Yuta, Niihori, Yoshiki, Mitsui, Masaaki, Kayahara, Eiichi, Yamago, Shigeru, Kobayashi, Kenji メールアドレス: 所属:
URL	<a href="http://hdl.handle.net/10297/00027756">http://hdl.handle.net/10297/00027756</a>

# Synthesis and Properties of a Cyclohexa-2,7-Anthrylene Ethynylene Derivative

Hironori Matsuki,<sup>[a]</sup> Keisuke Okubo,<sup>[a]</sup> Yuta Takaki,<sup>[a]</sup> Yoshiki Niihori,<sup>[b]</sup> Masaaki Mitsui,<sup>\*,[b]</sup> Eiichi Kayahara,<sup>[c]</sup> Shigeru Yamago,<sup>\*,[c]</sup> and Kenji Kobayashi<sup>\*,[a, d]</sup>

[a] H. Matsuki, K. Okubo, Dr. Y. Takaki, Prof. Dr. K. Kobayashi  
Department of Chemistry, Faculty of Science  
Shizuoka University  
836 Ohya, Suruga-ku, Shizuoka 422-8529 (Japan)  
E-mail: kobayashi.kenji.a@shizuoka.ac.jp

[b] Dr. Y. Niihori, Prof. Dr. M. Mitsui  
Department of Chemistry, College of Science  
Rikkyo University  
3-34-1, Nishiikebukuro, Toshima-ku, Tokyo 171-8501 (Japan)  
E-mail: mitsui@rikkyo.ac.jp

[c] Dr. E. Kayahara, Prof. Dr. S. Yamago  
Institute for Chemical Research  
Kyoto University  
Uji, Kyoto 611-0011 (Japan)  
E-mail: yamago@scl.kyoto-u.ac.jp

[d] Prof. Dr. K. Kobayashi  
Research Institute of Green Science and Technology  
Shizuoka University  
836 Ohya, Suruga-ku, Shizuoka 422-8529 (Japan)

Supporting information for this article is given via a link at the end of the document.

**Abstract:** The synthesis of a cyclohexa-2,7-(4,5-diaryl)anthrylene ethynylene **1** was achieved for the first time by using 1,8-diaryl-3,6-diborylanthracene and 1,8-diaryl-3,6-diiodoanthracene as key synthetic intermediates. Macrocycle **1** possesses a planar conformation of approximately  $D_{6h}$  symmetry, because of the triple bond linker between the anthracene units at the 2,7-positions. It was confirmed that macrocycle **1**, bearing bulky substituents at the outer peripheral positions, behaves as a monomeric form in solution without  $\pi$ -stacking self-association. Macrocycle **1** has an inner cavity size that allows specific inclusion of [9]cycloparaphenylene ([9]CPP), but not [8]CPP or [10]CPP, through aromatic edge-to-face CH- $\pi$  interaction.

## Introduction

Arylene macrocycles and arylene ethynylene macrocycles have attracted considerable attention in synthetic and physical organic chemistries, supramolecular chemistry, and materials science because of their unique structures and properties based on cyclic fully  $\pi$ -conjugated systems with an inner cavity.<sup>[1]</sup> In particular, cyclic *meta*-phenylene ethynylene hexamers<sup>[2]</sup> and cyclic 2,7-naphthylene ethynylene hexamers<sup>[3]</sup> possess approximately planar conformation and are expected to self-assemble into cofacial  $\pi$ -stacked aggregates such as nanofibers.<sup>[1a,c,d,e,2e,f]</sup> Anthracene derivatives function as a  $\pi$ -electronic core in a range of useful building blocks for optoelectronic applications such as fluorescent dyes,<sup>[4]</sup> organic electroluminescent devices,<sup>[5]</sup> two-photon absorption dyes,<sup>[6]</sup> emitters for triplet-triplet annihilation photon upconversion,<sup>[7]</sup> and organic semiconductors for organic field-effect transistors<sup>[8]</sup> and supramolecular architectures.<sup>[9]</sup> Therefore, the synthesis and characterization of cyclohexa-2,7-anthrylene (**1'''**), cyclohexa-2,7-

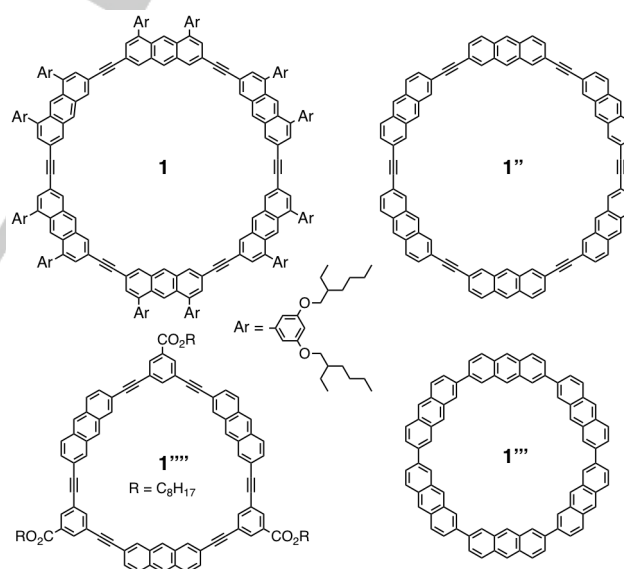
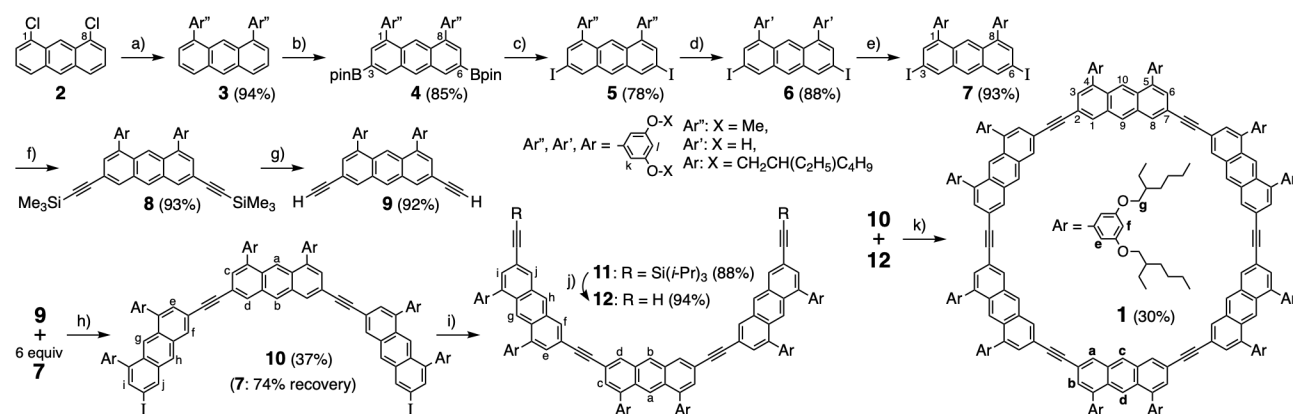


Chart 1. Structures of **1**, **1''**, **1'''**, and **1''''**.

anthrylene ethynylene (**1'''**), and their derivatives (Chart 1) would bring new perspective to the chemistry of arylene macrocycles and arylene ethynylene macrocycles directed to materials science and supramolecular chemistry. Recently, Toyota and co-workers reported the first synthesis of cyclohexa-2,7-anthrylene derivatives and inclusion of C<sub>60</sub> in the cavity.<sup>[10,11]</sup> We reported a cyclic arylene ethynylene hexamer composed of alternating 2,7-anthrylene ethynylene units and *meta*-phenylene ethynylene units (**1''''**) that self-associates through cofacial  $\pi$ -stacking interactions

## RESEARCH ARTICLE



**Scheme 1.** Synthetic Route of **1**. Reagents and conditions: a) 3,5-(MeO)<sub>2</sub>C<sub>6</sub>H<sub>3</sub>MgBr, NiCl<sub>2</sub>(PPh<sub>3</sub>)<sub>2</sub>, THF; b) (Bpin)<sub>2</sub>, [Ir(OMe)(COD)]<sub>2</sub>, dtbpy, cyclohexane; c) CuI, DMA; d) BBr<sub>3</sub>, CH<sub>2</sub>Cl<sub>2</sub>; e) 1-bromo-2-ethylhexane, K<sub>2</sub>CO<sub>3</sub>, KI, DMF; f) Me<sub>3</sub>SiCCH, PdCl<sub>2</sub>(PPh<sub>3</sub>)<sub>2</sub>, PPh<sub>3</sub>, CuI, THF–Et<sub>3</sub>N; g) K<sub>2</sub>CO<sub>3</sub>, CH<sub>2</sub>Cl<sub>2</sub>–MeOH; h) Pd(PPh<sub>3</sub>)<sub>4</sub>, CuI, THF–Et<sub>3</sub>N; i) *i*-Pr<sub>3</sub>SiCCH, Pd(PPh<sub>3</sub>)<sub>4</sub>, CuI, THF–Et<sub>3</sub>N; j) *n*-Bu<sub>4</sub>NF, CH<sub>2</sub>Cl<sub>2</sub>–THF; k) Pd(PPh<sub>3</sub>)<sub>4</sub>, CuI, THF–Et<sub>3</sub>N.

in solution and self-assembles into  $\pi$ -stacked nanofibers in a drop-cast film.<sup>[12,13]</sup> However, the synthesis of **1** and its derivatives, which are more extended  $\pi$ -conjugated aromatic system than **1**' and **1**'', is without precedent. As a part of our aim to synthesize cyclohexa-2,7-anthrylene ethynylene derivatives with the properties of self-assembled  $\pi$ -stacked nanofibers, we initially planned to investigate the monomeric properties of a cyclohexa-2,7-anthrylene ethynylene derivative without  $\pi$ -stacking. Here, we report the synthesis and properties of a soluble cyclohexa-2,7-(4,5-diaryl)anthrylene ethynylene **1** which behaves as a monomeric form in solution (Chart 1). Macrocycle **1** features an inner cavity size that is suitable for the specific inclusion of [9]cycloparaphenylene ([9]CPP), but not [8]CPP or [10]CPP, through aromatic edge-to-face CH– $\pi$  interaction.

## Results and Discussion

### Molecular Design and Synthesis of Macrocycle **1**

Unsubstituted **1**' would be insoluble in common organic solvents. We have designed cyclohexa-2,7-(4,5-diaryl)anthrylene ethynylenes as a soluble analogue of **1**', wherein the diaryl groups at the outer peripheral 4,5-positions of the anthracene unit do not infill the inner cavity and are expected to assist intermolecular cofacial  $\pi$ -stacking interaction of the macrocycle as well as formation of the self-assembled  $\pi$ -stacked nanofibers, suggested by CPK model consideration. On the other hand, to inhibit self-association of cyclohexa-2,7-(4,5-diaryl)anthrylene ethynylene through  $\pi$ -stacking, which would often make the purification of compounds difficult,<sup>[12]</sup> we chose 3,5-bis(2-ethylhexyloxy)phenyl group as the bulky diaryl groups. The synthesis of cyclohexa-2,7-(4,5-bis[3,5-bis(2-ethylhexyloxy)phenyl])anthrylene ethynylene (**1**) was achieved as shown in Scheme 1. The key reactions for the synthesis of **1** are the Ir-catalyzed regioselective direct diborylation of 1,8-diarylanthracene **3** to give **4**, followed by the CuI-mediated iododeboronation to give **5**. The use of **10** bearing iodo groups at both ends is essential for the synthesis of **1**.

The Kumada–Tamao–Corriu cross-coupling reaction of 1,8-dichloroanthracene **2**<sup>[14b]</sup> with 3,5-dimethoxyphenylmagnesium bromide gave **3**.<sup>[14]</sup> The Ir-catalyzed direct diborylation of **3**

occurred regioselectively at the 3,6-positions of the anthracene ring to give 1,8-diaryl-3,6-diborylanthracene **4** in 85% yield as a key synthetic intermediate.<sup>[15,16]</sup> The CuI-mediated iododeboronation of **4** produced 1,8-diaryl-3,6-diidoanthracene **5** in 78% yield,<sup>[17]</sup> whereas the reaction of **4** with NaI/chloramine-T gave complex mixture.<sup>[18]</sup> The demethylation of the methoxy groups of **5** followed by alkylation of the OH groups of the resulting **6** gave 1,8-bis[3,5-bis(2-ethylhexyloxy)phenyl]-3,6-diidoanthracene **7** as another key synthetic intermediate. The Sonogashira cross-coupling reaction of **7** with TMS-acetylene followed by desilylation of the resulting **8** gave 1,8-diaryl-3,6-diethynylanthracene **9**. The Sonogashira cross-coupling reaction of **9** with 6 equiv. of **7** gave triple-bond-linked linear anthracene trimer **10** bearing iodo groups at both ends in 37% yield.<sup>[19]</sup> The Sonogashira cross-coupling reaction of **10** with TIPS-acetylene followed by desilylation of the resulting **11** gave **12**, bearing ethynyl groups at both ends. Finally, the Sonogashira cross-coupling reaction of **10** with equimolar amount of **12** under high dilution conditions (0.5 mM each) produced macrocycle **1** in 30% yield.<sup>[20]</sup> The use of a combination of the linear anthrylene ethynylene trimers **10** and **12** as coupling partners facilitates the separation of **1** from the reaction mixture.<sup>[19]</sup> This coupling strategy would also have potential for the systematic synthesis of a variety of cyclohexa-2,7-(4,5-diaryl)anthrylene ethynylenes with various symmetries by changing the aryl groups of **10** and **12**.

The purification of **1** was carried out by short silica gel chromatography followed by recycling preparative HPLC (Figure S1). The structure of **1** was confirmed by <sup>1</sup>H and <sup>13</sup>C NMR spectroscopic (Figure S2) and MALDI-TOF-MS analyses (Figure S4). The <sup>1</sup>H NMR signal assignments of **1** were confirmed by 2D NOESY analysis (Figure S3). In this coupling reaction, the cyclododeca-2,7-(4,5-diaryl)anthrylene ethynylene or [2]catenane of **1** was also isolated in 9.3% yield as a side product (Figures S5–7).

### <sup>1</sup>H NMR Study of Macrocycle **1**

The <sup>1</sup>H NMR spectrum of macrocycle **1** shows a highly symmetrical species (Figure 1c and Figure S2a). The chemical shift of the <sup>1</sup>H NMR signals 'a', 'b', and 'c', which arise from the 1(8)-, 3(6)-, and 9-positions of the anthracene unit of **1**, respectively, remained almost unchanged irrespective of the concentration or solution temperature of **1** in CDCl<sub>3</sub> (Figures S8

## RESEARCH ARTICLE

and S9); however, signal 'd' at the 10-position of the anthracene unit was slightly shifted upfield upon increasing the solution temperature, probably because of a reduction in the deshielding effect of the diaryl groups at the 4,5-positions of the anthracene unit based on their rotation. If an anthracene-containing macrocycle with a planar conformation self-associates through cofacial  $\pi$ -stacking interaction, the  $^1\text{H}$  NMR signals of the anthracene unit would be expected to undergo an upfield shift upon decreasing the solution temperature as well as increasing the concentration of the macrocycle.<sup>[12]</sup> However, this is not the case for **1**. These results indicate that **1** behaves as a monomeric form in  $\text{CDCl}_3$  without  $\pi$ -stacking self-association, because **1** possesses the bulky 3,5-bis(2-ethylhexyloxy)phenyl groups at the outer peripheral 4,5-positions of the anthracene unit. Fluorescence emission spectra of **1** under various concentrations also support the conclusion that a monomeric form of **1** is present in  $\text{CH}_2\text{Cl}_2$  (Figure S14, see below).

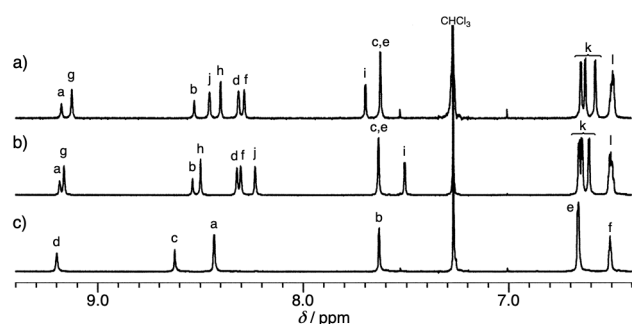


**Figure 1.** Comparison of  $^1\text{H}$  NMR spectra (400 MHz,  $\text{CDCl}_3$ , 298 K) of a) **10**, b) **12**, and c) **1** (1 mM). The signals marked "a–l" are assigned in Scheme 1.

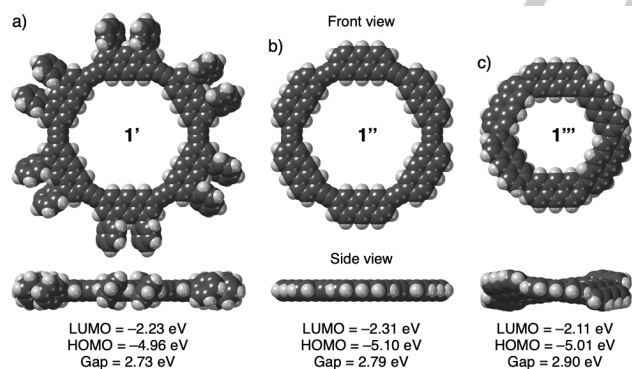


**Figure 2.** Ground-state optimized structures of a) cyclohexa-2,7-(4,5-diphenyl)anthrylene ethynylene (**1'**) as an analogue of **1**, b) cyclohexa-2,7-anthrylene ethynylene (**1''**), and c) cyclohexa-2,7-anthrylene (**1'''**) calculated at the B3LYP-DG3/6-31G(d) level.

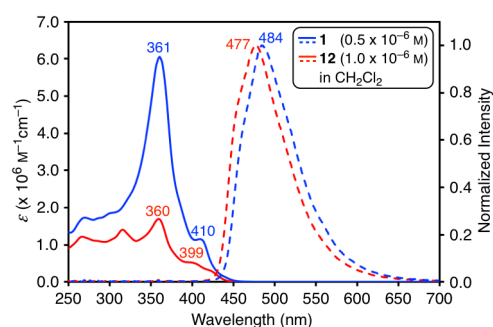
### Model Calculation of Macrocycle **1**

Figure 2 shows ground state ( $S_0$ ) optimized structures of cyclohexa-2,7-(4,5-diphenyl)anthrylene ethynylene (**1'**) as an analogue of **1**, cyclohexa-2,7-anthrylene ethynylene (**1''**), and cyclohexa-2,7-anthrylene (**1'''**) calculated at the B3LYP-DG3/6-31G(d) level. In contrast to **1'''**, with a nonplanar conformation of approximately  $S_6$  symmetry,<sup>[10a,b]</sup> macrocycles **1'** and **1''** possess a planar conformation of approximately  $D_{6h}$  symmetry, because of the triple bond linker between the anthracene units at the 2,7-

positions. HOMO–LUMO diagrams of **1'**, **1''**, and **1'''** are shown in Figure S10. Both the HOMO and LUMO energy levels of **1''** (–5.10 and –2.31 eV) were lower than those of **1'''** (–5.01 and –2.11 eV) through extension of the  $\pi$ -conjugation of **1''** compared with **1'''**. The HOMO energy level of **1'** (–4.96 eV) was higher than those of **1''** and **1'''**, whereas the LUMO energy level of **1'** (–2.23 eV) was between those of **1''** and **1'''**. The HOMO–LUMO energy gap decreased in the order **1'''** (2.90 eV) > **1''** (2.79 eV) > **1'** (2.73 eV). The orbital lobes of the HOMO and LUMO of **1'** and **1''** were relatively distributed more on the inside than on the outside of the cyclohexameric anthracene units compared with those of **1'''**, which were relatively distributed throughout the molecule (Figure S10).

### Photophysical and Electrochemical Properties of Macrocycle **1**

The UV–vis absorption and fluorescence emission spectra of cyclohexamer **1** ( $0.5 \times 10^{-6}$  M) and linear anthrylene ethynylene trimer **12** ( $1.0 \times 10^{-6}$  M) in  $\text{CH}_2\text{Cl}_2$  are shown in Figure 3, and their spectral data are summarized in Table S1. The UV–vis absorption maximum of **1** at  $\lambda_{\text{max}}(\text{abs}) = 361$  nm was almost the same as that of **12** ( $\lambda_{\text{max}}(\text{abs}) = 360$  nm), whereas the peak molar absorption coefficient of **1** was more than three times greater than that of **12**. The longest wavelength absorption maximum (shoulder peak) of **1** at  $\lambda_{\text{max}}(\text{abs}) = 410$  nm was redshifted by 11 nm relative to **12** ( $\lambda_{\text{max}}(\text{abs}) = 399$  nm), because of extension of the  $\pi$ -conjugation. Based on the time-dependent density functional calculation of **1''**, detailed assignments of the absorption spectrum of **1** were conducted, as shown in Figures S11–13 and Table S2. The shoulder peak at 410 nm mainly originates from the symmetry-allowed transitions from  $S_0$  to  $S_{4,5}$ . Although the electronic transitions from  $S_0$  to  $S_{1-3}$  are symmetry-forbidden, they could become weakly allowed transitions via vibronic couplings with the symmetry-allowed transitions. The strongest band at 361 nm corresponds to the symmetry-allowed transitions from  $S_0$  to  $S_{11}$ ,  $S_{12}$ ,  $S_{14}$ , and  $S_{15}$ . Based on the UV–vis absorption  $\lambda_{\text{cut-off}}$  (448 nm)<sup>[21]</sup> or the absorption onset ( $\lambda = 492$  nm) of **1** in  $\text{CH}_2\text{Cl}_2$ , the optical HOMO–LUMO energy gap was estimated to be 2.77 or 2.52 eV, respectively. These values are in good agreement with that obtained from the theoretical calculation of **1'** (2.73 eV).



**Figure 3.** The UV–vis absorption spectra (solid lines) and fluorescence emission spectra (dashed lines) of cyclohexamer **1** ( $0.50 \times 10^{-6}$  M, blue lines) and linear anthrylene ethynylene trimer **12** ( $1.0 \times 10^{-6}$  M, red lines) in  $\text{CH}_2\text{Cl}_2$ .

The fluorescence emission maximum of **1** at  $\lambda_{\text{max}}(\text{em}) = 484$  nm was redshifted by 7 nm relative to **12** ( $\lambda_{\text{max}}(\text{em}) = 477$  nm) (Figure 3). The absolute fluorescence quantum yields of **1** and **12**

## RESEARCH ARTICLE

were  $\Phi_F = 0.52$  and  $\Phi_F = 0.59$ , respectively. The shape and  $\lambda_{\max}(\text{em})$  of the fluorescence emission spectrum of **1** remained almost unchanged in  $\text{CH}_2\text{Cl}_2$  in the concentration range of  $0.5 \times 10^{-5}$  to  $0.5 \times 10^{-7}$  M (Figure S14). These results support the conclusion that **1** behaves as a monomeric form in solution without  $\pi$ -stacking self-association, as noted in the  $^1\text{H}$  NMR study described above. In contrast, the emission peak of **1** at  $\lambda_{\max}(\text{em}) = 484$  nm observed in  $\text{CH}_2\text{Cl}_2$  completely disappeared in the drop-cast film, and a new emission peak at  $\lambda_{\max}(\text{em}) = 538$  nm with  $\Phi_F = 0.08$  appeared (Figure S14). As **1** does not form  $\pi$ -stacked aggregates in solution due to the presence of bulky substituents, the observed new emission is most likely assigned to an excitonic emission.

Electrochemical analysis of macrocycle **1** was performed in a 0.1 M TBAPF<sub>6</sub> solution of THF (Figure S15). Cyclic voltammetry (CV) of **1** exhibited one irreversible oxidation wave and two pseudoreversible reduction waves. The oxidation and reduction potentials were determined to be 0.77 V and  $-1.77$  and  $-2.47$  V vs. the ferrocene/ferrocenium couple (Fc/Fc<sup>+</sup>) by differential pulse voltammetry (DPV). These results suggest that the oxidized **1** is not stable under the conditions used. The HOMO–LUMO energy gap was estimated to be 2.54 eV from the first oxidation and reduction potentials. This value is in good agreement with those obtained from the UV–vis absorption  $\lambda_{\text{cut-off}}$  or onset of **1** in  $\text{CH}_2\text{Cl}_2$  (2.77 or 2.52 eV), as mentioned above.

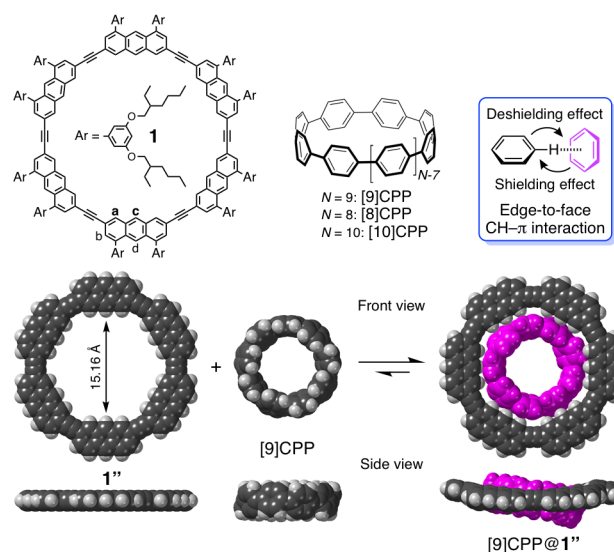


**Figure 4.** Association of macrocycle **1** with [9]CPP into [9]CPP@**1** through aromatic edge-to-face  $\text{CH}-\pi$  interaction. Optimized structure of [9]CPP@**1** calculated at the B3LYP-DG3/6-31G(d) level, wherein [9]CPP is shown in purple.

### Inclusion of [9]CPP in Macrocycle **1**

[*n*]Cycloparaphenylenes ([*n*]CPP: *n* = the number of *p*-phenylene units) have attracted considerable attention in physical organic chemistry and materials science because each [*n*]CPP represents a corresponding armchair carbon nanotube ((*n,n*)CNT) segment.<sup>[1f,g,i]</sup> Size-selective inclusion of [*n*]CPP in a host molecule is an important subject in relation to complexation, solubilization, and separation of CNT.<sup>[13c,22]</sup> We found that macrocycle **1** has an inner cavity with a size that is suitable for specific inclusion of [9]CPP, but not [8]CPP or [10]CPP,<sup>[23]</sup> to form a 1:1 inclusion complex [9]CPP@**1** through aromatic edge-to-face

$\text{CH}-\pi$  interaction (Figure 4).<sup>[10b,24]</sup> This is the first example for the inclusion of [*n*]CPP in a host molecule through aromatic edge-to-face  $\text{CH}-\pi$  interaction.<sup>[23]</sup> The inner cavity size of **1** is 15.16 Å including van der Waals (vdW) radius of hydrogen atoms (interatomic distance of diagonal two hydrogen atoms at the 9-position = 17.34 Å), calculated at the B3LYP-DG3/6-31G(d) level, whereas external diameters of [8]CPP, [9]CPP, and [10]CPP including vdW radius of carbon atoms are 14.53, 15.89, and 17.27 Å, respectively.<sup>[23,25]</sup> Thus, the inner cavity size of **1** fits the external diameter of [9]CPP, although the latter is slightly larger than the former. In a molecular model of [9]CPP@**1**, the geometry of [9]CPP in the cavity of **1** is inclined at ca. 11° angle with respect to the cavity mean plane of **1** and the shape of **1** is somewhat rolling to ease the tightness of the inclusion.

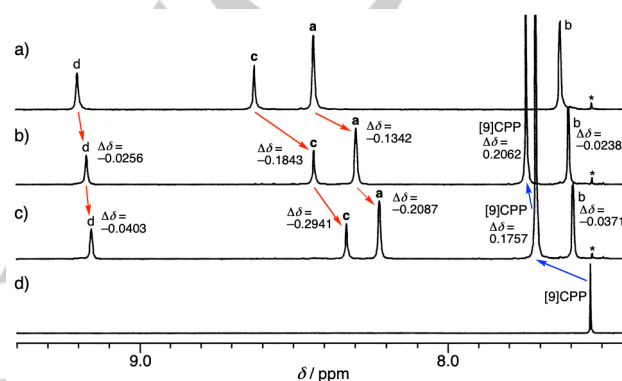


**Figure 5.** Association behavior of macrocycle **1** with [9]CPP monitored by  $^1\text{H}$  NMR (400 MHz,  $\text{CDCl}_3$ , 298 K): a) **1** alone (2.00 mM), b) a mixture of [**1**] = 2.00 mM and [[9]CPP] = 2.21 mM, c) a mixture of [**1**] = 2.00 mM and [[9]CPP] = 4.23 mM, and d) [[9]CPP] = 2.00 mM. The signals marked “a–d” are assigned in Figure 4. The chemical shift change ( $\delta_{\text{obsd}}$ ) of the signal of **1** (or [9]CPP) relative to the chemical shift ( $\delta_{\text{free}}$ ) of the signal of free **1** (or free [9]CPP) is defined as  $\Delta\delta = \delta_{\text{obsd}} - \delta_{\text{free}}$ . Asterisk is the satellite signal of the residual  $\text{CHCl}_3$ .

Figure 5 shows the  $^1\text{H}$  NMR spectra recorded upon the association of macrocycle **1** with [9]CPP in  $\text{CDCl}_3$  at 298 K, wherein the chemical shift change ( $\delta_{\text{obsd}}$ ) of the signal of **1** (or [9]CPP) relative to the chemical shift ( $\delta_{\text{free}}$ ) of the signal of free **1** (or free [9]CPP) is defined as  $\Delta\delta = \delta_{\text{obsd}} - \delta_{\text{free}}$ . The  $^1\text{H}$  NMR signals of the complex of **1** with [9]CPP ([9]CPP@**1**) and those of free **1** and free [9]CPP were observed as averaged signals, respectively. Under the conditions of [**1**] = 2.00 mM and [[9]CPP] = 2.21 mM (Figure 5b), the signals ‘a’, ‘b’, ‘c’, and ‘d’ at the respective 1(8)-, 3(6)-, 9-, and 10-positions of the anthracene unit of **1** were shifted upfield by 0.1342, 0.0238, 0.1843, and 0.0256 ppm, respectively, relative to those of free **1**, due to the shielding effect of the  $\pi$ -face of [9]CPP, whereas the signal of [9]CPP was shifted downfield by 0.2062 ppm relative to that of free [9]CPP, owing to the deshielding effect of the  $\pi$ -edge of **1**. Under the conditions of [**1**] = 2.00 mM and [[9]CPP] = 4.23 mM (Figure 5c), the signals ‘a’, ‘b’, ‘c’, and ‘d’ of **1** were shifted further upfield by 0.2087, 0.0371, 0.2941, and 0.0403 ppm, respectively, relative to those of free **1**, due to the increase of the complexation ratio of **1** with [9]CPP, whereas the signal of [9]CPP was shifted less downfield by 0.1757 ppm relative to that of free [9]CPP, owing to the addition of excess amount of [9]CPP relative to **1**. Upon complexation of **1** with [9]CPP, much larger upfield shifts of the signals ‘a’ and ‘c’ at the inner position of **1** relative to upfield shifts of signals ‘b’ and ‘d’

## RESEARCH ARTICLE

at the outer position of **1** clearly indicate that the inner cavity of **1** includes [9]CPP through aromatic edge-to-face CH– $\pi$  interaction (Figure 4). The  $^1\text{H}$  NMR signals of [9]CPP@**1**, free **1**, and free [9]CPP were not independently observed even at 223 K (Figure S16), indicating that the exchange of [9]CPP in and out of **1** is fast on the NMR time scale and that the geometry of [9]CPP included in the cavity of **1** is observed as an averaged form even at 223 K.

Upon mixing **1** with [8]CPP or [10]CPP, the chemical shifts of all species remained unchanged (Figures S17 and S18), indicating no association of **1** with these compounds. Thus, macrocycle **1** includes [9]CPP in the inner cavity in a size-specific manner.

The association constants ( $K_a$ ) of macrocycle **1** with [9]CPP to form a 1:1 inclusion complex [9]CPP@**1** in  $\text{CDCl}_3$  at 298–323 K were determined based on  $^1\text{H}$  NMR titrations monitoring the  $\Delta\delta$  values of the signals 'a' and 'c' of **1** (1.00 mM constant) as a function of the concentrations of [9]CPP (0–8.00 mM) at each temperature (Figure 6 and Figure S19) and the nonlinear least-square fitting analyses of the titration data (Figures S20–22). The results indicate the formation of a 1:1 complex of **1** with [9]CPP, and the  $K_a$  value at 298 K was estimated to be  $360 \pm 7 \text{ M}^{-1}$  for the signal 'a' ( $K_a = 350 \pm 6 \text{ M}^{-1}$  for the signal 'c').<sup>[26]</sup> The thermodynamic parameters for the association of macrocycle **1** with [9]CPP in  $\text{CDCl}_3$  were estimated to be  $\Delta H = -4.24 \text{ kcal mol}^{-1}$  and  $\Delta S = -2.52 \text{ cal mol}^{-1} \text{ K}^{-1}$  for the signal 'a' ( $\Delta H = -3.99 \text{ kcal mol}^{-1}$  and  $\Delta S = -1.79 \text{ cal mol}^{-1} \text{ K}^{-1}$  for the signal 'c'), indicating an enthalpically driven association (Figure S23). Thus, aromatic edge-to-face CH– $\pi$  interaction serves as an attractive force for the formation of [9]CPP@**1**.<sup>[10b, 24b]</sup> The unfavorable entropy term arises from the decreased number of particles and the decreased molecular freedom by the complex formation from two independent **1** and [9]CPP.

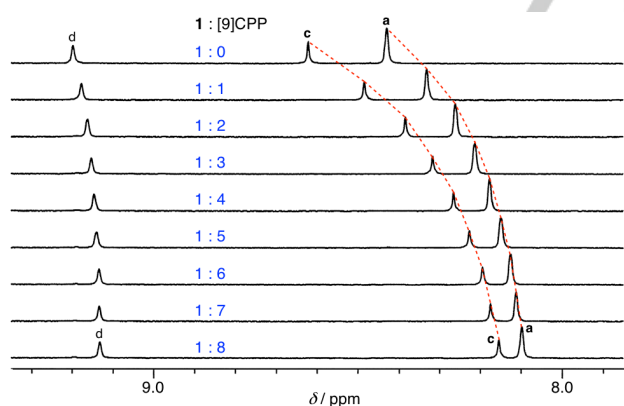


**Figure 6.**  $^1\text{H}$  NMR spectra (400 MHz) of the titration for the association of macrocycle **1** (1.00 mM constant) with [9]CPP (0–8.00 mM) in  $\text{CDCl}_3$  at 298 K. The signals marked "a, c, and d" are assigned in Figure 4.

## Conclusion

We have achieved the first synthesis of cyclohexa-2,7-(4,5-diaryl)anthrylene ethynylene **1**. Macrocycle **1**, with bulky substituents at the outer peripheral positions, behaves as a monomeric form in solution without  $\pi$ -stacking self-association. Macrocycle **1** has an inner cavity size that specifically includes [9]CPP, but not [8]CPP or [10]CPP, through aromatic edge-to-face CH– $\pi$  interaction. Macrocycle **1** has potential as an agent for

solubilization, separation, and purification of CNT by formation of a pseudo-polyrotaxane.<sup>[13c, 22]</sup> A study for the systematic synthesis of various cyclohexa-2,7-(4,5-diaryl)anthrylene ethynylene derivatives directed to self-assembled  $\pi$ -stacked nanofibers and functional materials, by changing the aryl groups of **10** and **12**, is a next subject in our laboratory.

## Acknowledgements

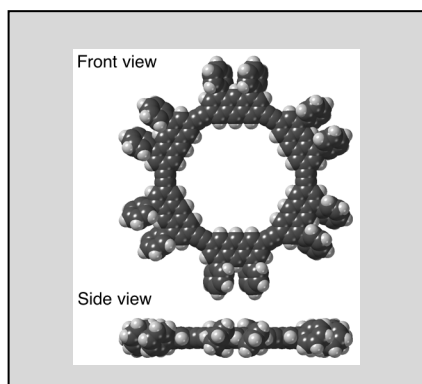
We thank Prof. Shigehisa Akine, Kanazawa University, for TitrationFit (program for analysis of host-guest complexation). Theoretical calculations were performed using Research Center for Computational Science, Okazaki, Japan. Financial supports from JSPS, KAKENHI Grant No. 25620029 (K.K.) and 16H06352 (S.Y.) are gratefully acknowledged.

**Keywords:** arenes • conjugation • host-guest systems • macrocycles •  $\pi$  interactions

- [1] a) W. Zhang, J. S. Moore, *Angew. Chem. Int. Ed.* **2006**, *45*, 4416–4439; *Angew. Chem.* **2006**, *118*, 4524–4548; b) T. Kawase, H. Kurata, *Chem. Rev.* **2006**, *106*, 5250–5273; c) L. Zang, Y. Che, J. S. Moore, *Acc. Chem. Res.* **2008**, *41*, 1596–1608; d) S. Höger, *Pure Appl. Chem.* **2010**, *82*, 821–830; e) M. Iyoda, J. Yamakawa, M. J. Rahman, *Angew. Chem. Int. Ed.* **2011**, *50*, 10522–10553; *Angew. Chem.* **2011**, *123*, 10708–10740; f) S. Yamago, E. Kayahara, T. Iwamoto, *J. Synth. Org. Chem. Jpn.* **2014**, *72*, 992–1005; g) Y. Segawa, A. Yagi, K. Matsui, K. Itami, *Angew. Chem. Int. Ed.* **2016**, *55*, 5136–5158; *Angew. Chem.* **2016**, *128*, 5222–5245; h) Z. Sun, T. Matsuno, H. Isobe, *Bull. Chem. Soc. Jpn.* **2018**, *91*, 907–921; i) S. Toyota, E. Tsurumaki, *Chem. Eur. J.* **2019**, *25*, 6878–6890; j) Y. Xu, M. von Delius, *Angew. Chem. Int. Ed.* **2020**, *59*, 559–573; *Angew. Chem.* **2020**, *132*, 567–582; k) K. Miki, K. Ohe, *Chem. Eur. J.* **2020**, *26*, 2529–2575.
- [2] a) S. Lahiri, J. L. Thompson, J. S. Moore, *J. Am. Chem. Soc.* **2000**, *122*, 11315–11319; b) Y. Tobe, N. Utsumi, K. Kawabata, A. Nagano, K. Adachi, S. Araki, M. Sonoda, K. Hirose, K. Naemura, *J. Am. Chem. Soc.* **2002**, *124*, 5350–5364; c) D. Zhao, J. S. Moore, *Chem. Commun.* **2003**, 807–818; d) S. Höger, X. H. Cheng, A.-D. Ramminger, V. Enkelmann, A. Rapp, M. Mondeshki, I. Schnell, *Angew. Chem. Int. Ed.* **2005**, *44*, 2801–2805; *Angew. Chem.* **2005**, *117*, 2862–2866; e) D. Suzuki, H. Abe, M. Inouye, *Org. Lett.* **2016**, *18*, 320–323; f) Y. L. Zhong, Y. Yang, Y. Shen, W. W. Xu, Q. H. Wang, A. L. Connor, X. B. Zhou, L. He, X. C. Zeng, Z. F. Shao, Z. L. Lu, B. Gong, *J. Am. Chem. Soc.* **2017**, *139*, 15950–15957.
- [3] H. Sugiura, Y. Takahira, M. Yamaguchi, *J. Org. Chem.* **2005**, *70*, 5698–5708.
- [4] Y. Fujiwara, R. Ozawa, D. Onuma, K. Suzuki, K. Yoza, K. Kobayashi, *J. Org. Chem.* **2013**, *78*, 2206–2212.
- [5] W. Nakanishi, S. Hitosugi, A. Piskareva, Y. Shimada, H. Taka, H. Kita, H. Isobe, *Angew. Chem. Int. Ed.* **2010**, *49*, 7239–7242; *Angew. Chem.* **2010**, *122*, 7397–7400.
- [6] a) H. C. Zhang, E. Q. Guo, Y. L. Zhang, P. H. Ren, W. J. Yang, *Chem. Mater.* **2009**, *21*, 5125–5135; b) Y. Hirumi, K. Tamaki, T. Namikawa, K. Kamada, M. Mitsui, K. Suzuki, K. Kobayashi, *Chem. Asian J.* **2014**, *9*, 1282–1290.
- [7] a) P. Duan, N. Yanai, H. Nagatomi, N. Kimizuka, *J. Am. Chem. Soc.* **2015**, *137*, 1887–1894; b) K. Kamada, Y. Sakagami, T. Mizokuro, Y. Fujiwara, K. Kobayashi, K. Narushima, S. Hirata, M. Vacha, *Mater. Horiz.* **2017**, *4*, 83–87.
- [8] a) H. Meng, F. Sun, M. B. Goldfinger, F. Gao, D. J. Londono, W. J. Marshal, G. S. Blackman, K. D. Dobbs, D. E. Keys, *J. Am. Chem. Soc.* **2006**, *128*, 9304–9305; b) C. Xu, P. He, J. Liu, A. Cui, H. Dong, Y. Zhen, W. Chen, W. Hu, *Angew. Chem. Int. Ed.* **2016**, *55*, 9519–9523; *Angew. Chem.* **2016**, *128*, 9671–9675; c) Y. Takaki, Y. Wakayama, Y. Ishiguro, R. Hayakawa, M. Yamagishi, T. Okamoto, J. Takeya, K. Yoza, K. Kobayashi, *Chem. Lett.* **2016**, *45*, 1403–1405.

- [9] M. Yoshizawa, J. K. Klosterman, *Chem. Soc. Rev.* **2014**, *43*, 1885-1898.
- [10] For cyclohexa-2,7-anthrylene derivatives, see: a) Y. Yamamoto, K. Wakamatsu, T. Iwanaga, H. Sato, S. Toyota, *Chem. Asian J.* **2016**, *11*, 1370-1375; b) Y. Yamamoto, E. Tsurumaki, K. Wakamatsu, S. Toyota, *Angew. Chem. Int. Ed.* **2018**, *57*, 8199-8202; *Angew. Chem.* **2018**, *130*, 8331-8334; c) M. D. Giovannantonio, X. Yao, K. Eimre, J. I. Urgel, P. Ruffieux, C. A. Pignedoli, K. Müllen, R. Fasel, A. Narita, *J. Am. Chem. Soc.* **2020**, *142*, 12046-12050.
- [11] For cyclotetra-2,6-anthrylene, see: J. Wang, G. Zhuang, M. Chen, D. Lu, Z. Li, Q. Huang, H. Jia, S. Cui, X. Shao, S. Yang, P. Du, *Angew. Chem. Int. Ed.* **2020**, *59*, 1619-1626; *Angew. Chem.* **2020**, *132*, 1636-1643.
- [12] Y. Takaki, R. Ozawa, T. Kajitani, T. Fukushima, M. Mitsui, K. Kobayashi, *Chem. Eur. J.* **2016**, *22*, 16760-16764.
- [13] For arylene ethynylene macrocycles containing 9,10-anthrylene ethynylene units, see: a) K. Miyamoto, T. Iwanaga, S. Toyota, *Chem. Lett.* **2010**, *39*, 288-290; b) K. Miki, M. Fujita, Y. Inoue, Y. Senda, T. Kowada, K. Ohe, *J. Org. Chem.* **2010**, *75*, 3537-3540; c) K. Miki, K. Saiki, T. Umeyama, J. Baek, T. Noda, H. Imahori, Y. Sato, K. Suenaga, K. Ohe, *Small* **2018**, *14*, 1800720.
- [14] a) K. Tamao, K. Sumitani, M. Kumada, *J. Am. Chem. Soc.* **1972**, *94*, 4374-4376; b) H. O. House, J. A. Hrabie, D. VanDerveer, *J. Org. Chem.* **1986**, *51*, 921-929.
- [15] For Ir-catalyzed direct diborylation of acenes, see: a) D. N. Coventry, A. S. Batsanov, A. E. Goeta, J. A. K. Howard, T. B. Marder, R. N. Perutz, *Chem. Commun.* **2005**, 2172-2174; b) T. Kimoto, K. Tanaka, Y. Sakai, A. Ohno, K. Yoza, K. Kobayashi, *Org. Lett.* **2009**, *11*, 3658-3661; c) Y. Takaki, K. Yoza, K. Kobayashi, *Chem. Lett.* **2017**, *46*, 655-658.
- [16] The Ir-catalyzed direct diborylation of 1,8-bis(*p*-hexylphenyl)anthracene, 1,8-bis(*p*-(*n*-octyloxy)phenyl)anthracene, and 1,8-bis(*p*-(methoxycarbonyl)phenyl)anthracene also occurred regiospecifically at the 3,6-positions of the anthracene ring to give 1,8-diaryl-3,6-diborylanthracenes in 93%, 77%, and 66% yields, respectively, whereas the borylation did not occur at the *p*-substituted-phenyl groups in these compounds.
- [17] The reaction of **4** with CuI (8 equiv.) in dry DMF at 80 °C for 2 d under dry air (modified Murafuji's method) in place of our reaction condition (in dry DMA at 80 °C for 3 d under Ar) gave **5** in 55% yield. M. Narita, T. Murafuji, S. Yamashita, M. Fujinaga, K. Hiyama, Y. Oka, F. Tani, S. Kamijo, K. Ishiguro, *J. Org. Chem.* **2018**, *83*, 1298-1303.
- [18] G. Battagliarin, C. Li, V. Enkelmann, K. Müllen, *Org. Lett.* **2011**, *13*, 3012-3015.
- [19] The Sonogashira cross-coupling reaction of monomer **9** with equimolar amount of monomer **7** showed the formation of linear oligomers such as 5, 6, 7-mers and so on in addition to a trace amount of **1**, which made it difficult to separate **1** from the reaction mixture.
- [20] The use of **10** is essential for the synthesis of **1**. The coupling reaction of the analogue of **10** bearing bromo groups at both ends (**10'**) with **12** showed the butadiyne-connected oligomerization of **12** and almost quantitative recovery of **10'**.
- [21] Wavelength at which the transmittance is 95% relative to the absorbance of  $\lambda_{\max}(\text{abs}) = 410 \text{ nm}$ .
- [22] a) E. M. Pérez, *Chem. Eur. J.* **2017**, *23*, 12681-12689; b) S. Selmani, D. J. Schipper, *Chem. Eur. J.* **2019**, *25*, 6673-6692.
- [23] For inclusion of [n]CPP in [n + 5]CPP through cofacial  $\pi$ -stacking interaction, see: S. Hashimoto, T. Iwamoto, D. Kurachi, E. Kayahara, S. Yamago, *ChemPlusChem* **2017**, *82*, 1015-1020.
- [24] a) M. Nishio, *Phys. Chem. Chem. Phys.* **2011**, *13*, 13873-13900; b) T. Matsuno, M. Fujita, K. Fukunaga, S. Sato, H. Isobe, *Nature Commun.* **2018**, *9*, 3779.
- [25] T. Iwamoto, Y. Watanabe, Y. Sakamoto, T. Suzuki, S. Yamago, *J. Am. Chem. Soc.* **2011**, *133*, 8354-8361.
- [26] Relatively small  $K_a$  of **1** with [9]CPP to form [9]CPP@**1** in CDCl<sub>3</sub> and the fast exchange of [9]CPP in and out of **1** on the NMR time scale hampered measurements of DOSY and 2D NOESY spectra and elucidation of the photophysical properties of [9]CPP@**1**.

## Entry for the Table of Contents



**Extended  $\pi$ -conjugated macrocycle:** The synthesis of a cyclohexa-2,7-anthrylene ethynylene derivative was achieved for the first time. This macrocycle possesses a planar conformation and an inner cavity that includes [9]cycloparaphenylene through aromatic edge-to-face CH- $\pi$  interaction.